Signal analysis to study the impact of tongue roughness on oral friction mechanisms with a custom-built tribometer

Miodrag Glumac, Véronique Bosc, Paul Menut, Marco Ramaioli, Frederic Restagno, Sandrine Mariot, Vincent Mathieu

Signal analysis to study the impact of tongue roughness on oral friction mechanisms with a custom-built tribometer

Miodrag Glumac[a], Véronique Bosc[a], Paul Menut[a], Marco Ramaioli[a], Frédéric Restagno[b], Sandrine Mariot[b], Vincent Mathieu[a,*]

[a] Université Paris-Saclay, INRAE, AgroParisTech, UMR SayFood, 91120, Palaiseau, France

[b] Université Paris-Saclay, CNRS, Laboratoire de Physique des Solides, 91400, Orsay, France

*Corresponding author:

Vincent Mathieu

Paris-Saclay Food and Bio-product Engineering Research Unit (SayFood UMR 782)

Paris Saclay, INRAE, AgroParisTech

22, place de l'Agronomie

91120 Palaiseau, France

Email: vincent.mathieu@inrae.fr

Abstract

A custom-built tribometer was employed to investigate the impact of the roughness of deformable tongue mimicking surfaces (TMS) on friction mechanisms occurring under the effect of lubrication with Newtonian solutions of glycerol. TMSs with modulated roughness (range of asperity heights Ra: 20-140 µm) were manufactured from gels of polyvinyl alcohol (PVA). Newtonian aqueous solutions of glycerol covering a wide range of viscosity (1-1400 mPa.s) were used as simple food models spread on the TMSs. The tribological behavior of the system was studied during shear back and forth movements. The ratio between tangential and normal forces was analyzed both in terms of average values and of fluctuations, over specific time periods set at the end of motion and rest steps. The average values of friction level were reported to increase when (i) the roughness of the TMSs increased and when (ii) the viscosity of glycerol solutions decreased. These trends could be consistent with mixed lubrication. The fluctuations of friction level during motion steps were for their part generally of higher amplitude as the roughness of the surface increased, with main frequencies ranging from 10 to 20 Hz. The study demonstrates the importance (i) of the biological relevance of tongue properties (contact areas, rigidity, and asperity heights) and (ii) of the thorough analysis of tangential to normal force ratio to better understand the complex mechanisms of friction occurring in the mouth during food consumption.

Keywords: Food oral processing; Texture perception; Oral tribology; Biomimicry; Tongue roughness; Food viscosity.

1. Introduction

Texture perceptions of food encompass multiple sensory stimuli associated with the structural and mechanical properties of food [1,2]. In particular, tactile features sensed when food interacts with oral surfaces are among the main focuses of food texture investigations [3]. Complementary to sensory analysis, the understanding of the physical and mechanical phenomena that can impact texture perceptions requires the development of experimental approaches that integrate both the characteristics of the food and the complex properties of the organs involved during oral processing [4]. Various prototypes attempting to more or less completely mimic all the stages of food oral processing have thus been designed in recent years [5]. Among these different stages, food manipulation by the tongue has been the subject of particular attention [6]. Indeed, the tongue allows the continuous evaluation of the mechanical transformations undergone by the food while guiding it towards the different organs of the mouth to unfold the strategy making it possible to obtain a food bolus ready to be swallowed under safe and comfortable conditions.

In particular, oral tribology approaches have been deployed to unravel thin-film lubrication phenomena and to try to uncover relevant friction factors and events that happen between the tongue and the palate during eating [7,8]. Systematic and comprehensive reviews explained in depth the current understanding of oral tribological investigations and their influence on sensory perceptions [9,10]. The importance of emulating more closely real oral conditions was well highlighted. To achieve these objectives, it is necessary to go beyond the classic framework allowed by commercial tribology devices, either by adapting them or by designing completely new ones. Taking into account the complex properties of the tongue is a recognized prerequisite to realistically address the tribological behavior of food [11,12].

Accounting for tongue rigidity led to significant growth in oral tribology studies in recent years, in particular with the use of PDMS as the most widespread substrate [13]. Human tongue's elastic modulus has been measured to be around 10 kPa at rest and 120 kPa when contracted [6]. With cryogels of polyvinyl alcohol (PVA), our group has chosen a material that allows reaching a few tens of kPa (thus sticking at best to physiological orders of magnitude) [14]. The hydrophilic character of PVA gels (they are largely composed of water) [15] gives them wettability properties which are relevant compared to those of the tongue. This is thus an additional advantage of PVA gels to the detriment of PDMS, insofar as friction properties have been shown to be highly influenced by the hydrophobicity of the tribopairs [16]. The complex nature of tongue motions during friction with the palate also led some authors to the consideration of not only linear but also circular or elliptical motions which were shown to drastically influence friction properties [17]. Finally, we can note a growing interest in the role of saliva on oral friction for various applications, such as the development of thickeners to treat dysphagia problems [18], the use of oral care products [19], as well as for understanding food oral processing [20].

Current emerging trends are to take into account the complex topographical properties of the tongue induced by the lingual papillae that cover the tongue's surface [21]. In a recent study, tongue roughness properties measured in human volunteers were related to lubrication behaviors and smoothness perception [22]. In studies focused on uniaxial compressions between tongue and palate, the roughness of the tongue has been identified as a key parameter that can influence the distribution and transmission of mechanical stresses at the tongue-palate interface, but also the spreading patterns of the fluids located at the interface [23,24].

Tongue roughness insights are also implemented in various custom tribological instruments to make them more in line with oral conditions [7,25]. More generally, the effect of surface roughness of soft tribopairs made of hydrogels has been the subject of different studies which are not limited to food science applications but are also of interest to communities of biomedical engineering, bioscience, or even soft robotics. Under lubrication with water, smooth PVA hydrogels with varied rigidity have been paired with rigid glass substrates with different roughness properties, demonstrating a velocity dependence of friction attributed to surface contact dynamics [26]. Roughness has also been considered directly on hydrogels that were paired with smooth glass surfaces [27]. Confocal laser microscopy was used to visualize the different contact behaviors at the interface. The differences in lubrication regimes observed between smooth and rough gels were shown to diminish when the normal load increased.

Friction phenomena have also been investigated between tribopairs both made up of soft hydrogels of different natures, and submerged in water [28]. The system consisted of hemispherical probes and flat substrates with varied roughness properties obtained by molding on sandpaper sheets (grit size varying between 8 and 200 µm, which makes sense in relation to the topographic characteristics of the tongue). Conducted under physiologically relevant conditions for tongue-palate interactions (shearing velocity of 20 $mm.s^{-1}$, normal pressure up to 7 kPa), this work revealed two friction regimes. In the first regime, corresponding to low normal loads, friction was shown to vary with surface roughness and hydrogels' stiffness. Beyond a certain threshold of contact pressure, a second friction regime attributed to smoothening of asperities led to a constant friction coefficient and was shown to be constant across roughness, and found to be material dependent. More recently, two papers proposed original 3-D printing of molds to generate soft substrates with controlled roughness [29,30]. The asperities were made up of cylindrical pillars whose height, diameter, and density could be custom-designed, following different symmetrical arrangement diagrams for their patterning. In the first paper, the tribopair was composed of a rigid spherical probe paired with texturized PDMS substrates, in presence of suspensions of particles in mixtures of water and glycerol [30]. The area density of pillars was shown to promote lubrication, while distinct frictional behaviors were reported when the rigidity of the particles was varied. In the second one, the substrates were paired with a soft hemispherical probe submerged in water which made it possible to show the importance of the morphology and the overall spatial patterning of the asperities in the case of gel-gel friction. The bending and the density of the pillars were identified as important factors having an impact on the effective contact surface between the probe and the substrate, and on subsequent friction phenomena. The surface of the probe which effectively interacts with the substrate also has to be taken into account and compared with the dimensions of the asperities.

These different studies are essential to understand friction mechanisms involving rough hydrogels. Nevertheless, most of these studies are based on the use of rheometers with rotational geometries involving hemispherical probes on flat substrates. To explore contact surfaces that are more representative of the contact between the tongue and the palate, new tribological systems must therefore be designed and deployed. The implementation of tongue roughness in oral tribology studies thus led to the consideration of new tribopairs with increased surface area, leading to improved physiological relevance and paving the way for investigating the behavior of complex and heterogeneous food models (e.g. presence of particles, mixtures of phases). It is in particular for this purpose that a new custom-built tribometer was designed and presented by our group in a recent publication [14]. The device allows the generation of a contact area of approximately 10 cm^2 between the artificial tongue and palate, which is almost half of the total surface of the hard palate, estimated at around 20 cm^2 [31]. Such a configuration thus offers improved physiological relevance, when compared to that of conventional commercial tribopairs. Still, with the aim of closer emulating in-mouth conditions, the use of two orthogonal translation stages makes it possible to impose complex sequences of movements, combining simultaneously both compression and shearing, exactly as we do when we eat. This marks the main originality of our approach in the general context of the growing scientific community's interest in soft tribology applied to food oral processing. The proof-of-concept publication made it possible to perform a first scan of the different operational factors that can be varied on the newly designed device. The importance of the normal force and shear velocity parameters on the friction phenomena could logically be highlighted [14]. Before going further with complex sequences mixing compressional and shearing motions, this newly designed in-house equipment requires going through validation stages through simplified protocols, in order to test and approve more in depth the reliability of the extracted data. This is all the more important since, as underlined in a recent review, each tribology system has its specificities, making comparisons between studies complicated [13].

For this, we propose to explore the benefits to be drawn from this custom-made system, which provides access to raw force signal data and thus offers all degrees of freedom for analyzing them as finely as desired. Unlike conventional commercial tribometers, the analysis is thus not restricted to the friction coefficient measured in steady state dynamics. It is also possible to analyze the transient phases, or to study the characteristics of fluctuations over time, as a few rare but very interesting articles have done [32].

In the present study, the objective is thus to implement the custom build tribometer previously introduced by our team, to characterize in an original way the impact of the roughness properties of the tongue on the phenomena of friction against the palate. Tongue mimicking surfaces covering physiologically relevant ranges of roughness asperity heights were designed and implemented on the device. Cycles alternating between shearing motions and rest phases were thus imposed between tongue mimicking surfaces and an aluminum plate mimicking the human hard palate. Constant conditions of shearing velocity and normal force were imposed, and the use of Newtonian solutions of glycerol covering a wide spectrum of viscosities (representative of that of the liquid and semi-liquid foods that we consume) made it possible to vary the lubrication regime. Original processing methods were implemented to analyze the ratio between tangential and normal forces, both in terms of levels of amplitude and of fluctuations during dynamic friction steps, but also in terms of residual levels during rest periods.

2. Material and methods

2.1. Newtonian solutions of glycerol

Newtonian solutions of glycerol were prepared and used as lubricants for the tribological measurements. As the experiments were conducted with fixed shear velocity and normal force, varying the viscosity of the solutions made it possible to change the lubrication regime and move along the Stribeck curve. Mixtures of glycerol (purity ≥ 99.0%, Thermo Fisher Scientific, Waltham, MA, USA) and water were considered. Six solutions were prepared in total, labeled based on their glycerol content (w/w %): G_{100} (pure glycerol), G_{97}, G_{93}, G_{85}, G_{50}, and G_0 (water). Concentration levels were defined based on literature data, in order to have a progressive graduation of the viscosity level between G_0 (the thinnest) and G_{100} (the thickest) [33]. Water was added to glycerol in glass containers and placed under magnetic mixing for 30 minutes. The viscosity of the obtained solutions was measured on a rheometer (Physica MCR 301, Anton Paar, GmbH, Austria) with concentric cylinders (CC27/T200/SS), at 20° C.

The well-known and established Newtonian behavior was checked through logarithmically increasing and decreasing shear rates (1-1000 s^{-1}). The average and standard deviation values of viscosity at 50 s^{-1} obtained after five replications are provided in Table 1, 50 s^{-1} being recommended in the literature as a relevant shear rate for food oral processing [34]. A well-known non-linear behavior of viscosity versus glycerol concentration was confirmed (exponential trend).

Table 1. *Viscosity of glycerol and water mixtures measured at 50 s^{-1} shear rate and 20° C temperature. Standard deviation values were below 10^{-2} mPa.s and G_0 value (water) was taken from a literature report* [35].

Solution label	G_0	G_{50}	G_{85}	G_{93}	G_{97}	G_{100}
Viscosity (mPa.s)	1	6	106	351	728	1352

2.2. Manufacturing and characterization of Tongue Mimicking Surfaces (TMSs)

Six types of Tongue Mimicking Surfaces (TMSs) were designed, each one corresponding to a given level of roughness. TMSs were made from polyvinyl alcohol (PVA) cryogels. PVA (MW 89,000–98,000, 99% hydrolyzed, Sigma Aldrich, Saint-Louis, USA) was dissolved in water (10%, w/w), heated to 80 °C and kept under magnetic steering for a duration of 2 h. The obtained solution was then poured in rectangular parallelepiped molds (dimensions: length 80 mm, width 45 mm, thickness 25 mm). The objective was to prepare TMSs with asperities in a range that is reminiscent of human tongue asperity heights [36,37]. The roughness was obtained by covering the bottom face of the molds (80 × 45 mm) with sandpaper (Leman, Saint-Clair-de-la-Tour, France) with varied classes of grain sizes: P_{24}, P_{36}, P_{40}, $P_{80,}$ and P_{100} (defined by the Federation of European Producers of Abrasives). These classes correspond to the number of meshes per inch square of sieve surface used to size the grains: the higher the class number, the smaller the grain size and the smoother the surface. A silicone sheet was used to prepare the last TMS. Such surface had a qualitative visual appearance that appeared smoother than the smoothest sandpaper sheet considered. The molds filled with PVA solution underwent a total of two freezing and thawing cycles, thus allowing the solutions to gel with the desired rigidity [38]. The freeze steps were done at −20 °C in a cold storage room (Isobar N.V., Belgium) and lasted 16 h, while the thawing ones lasted 8 h in the air-conditioned laboratory kept at 20° C. After unmolding, TMSs were all stored under the same conditions: they were placed in hermetic boxes, immersed in water, and maintained at ambient laboratory temperature (20°C). Under these conditions, PVA cryogels can be stored for several months without their mechanical properties to be altered. In the present case, a week passed after the manufacture of the TMSs, before the start of the experiments. Then, all the experiments were carried out over a period of about a month.

A texture analyzer (TA.XTplus, Stable Micro System, Surrey, United Kingdom) was used to measure the Young's modulus on two out of the six TMSs (the smoothest and the roughest). A planar circular probe with dimensions greater that the surface of the TMSs was used. The protocol was a strain rate of 5%, with a compression speed of 10 $mm.s^{-1}$ (six replicates per TMS). The slope of the stress-strain curve was assessed during both the loading and unloading phases of the test. The stiffness values obtained during the loading and unloading phases were respectively 29.4 ± 1.0 kPa and 30.2 ± 0.5 kPa for the roughest TMS, and 31.8 ± 0.2 kPa and 30.6 ± 0.2 kPa for the smoothest. No major differences could be noted between both samples, confirming that all TMSs had the same rigidity.

The roughness of the TMSs was analyzed by profilometry (DektakXT®, Bruker, USA). Tested samples included one TMS per class of roughness (six samples). Three one-dimensional profiles were performed for each TMS analyzed (each was 30 mm long), with a 45° rotation between one profile and the next, in order to cover as well as possible the area of interest for tribology measurements. The profilometry probe was a stylus with a 2 µm radius, the force was

1 mg, and the achieved resolution was 1.66 µm/pt, at a constant speed of 500 $µm.s^{-1}$. The data from each one-dimensional profile (signals of the measured asperity height as a function of the tip scan distance) was processed individually on MATLAB (The MathWorks, Natick, Massachusetts, USA). On the 1-D profiles, the absence of qualitative differences between the slopes of the ascending and descending phases of the indenter suggested that the settings have made it possible to limit potential scratching effects. The processing of the profiles and the calculation of the roughness parameters were carried out following the instructions provided in the ISO 4287 standard. Filters were applied on the raw measured surface profiles to isolate the waviness from the roughness components of the profiles (the first one being due to a lack of flatness and not to the shape of asperities). The cut-off length λ_c used in the filter was set to 10 mm, which is ten times higher that the highest grain size of the coarsest sandpaper used, and which also corresponds to the course of shear motions implemented for the tribological tests described hereafter. Two main roughness parameters were calculated from the filtered profiles: the arithmetical mean height (Ra) and the mean width of the profile elements (RSm). Ra is the arithmetic average of the deviations from the mean line of the surface profiles, calculated over the whole length of the one-dimensional scan. The Ra parameter is therefore linked to the vertical amplitude of the roughness. RSm for its part was calculated as the average value of the distance between the changes of sign of the height of the profiles (crossing of the average height). This parameter, therefore, provides information on the width of the asperities. The mean and standard deviations of Ra and RSm values obtained from the three one-dimensional scans performed on each TMS were then calculated.

In addition to the one-dimensional measurements, for each of the six roughness levels studied, two-dimensional measurements were performed with the same profilometry equipement, consisting of 125 successive one-dimensional profiles performed with the same settings. With a spacing of 20 µm between each profile, it was possible to cover a surface of 2.5 × 3.0 mm, to have two-dimensional representations for the qualitative visualization of the surface morphology.

2.3. Custom-buit tribometer

The custom-built tribometer used in this study was previously described in detail in a recent proof of concept study [14]. A schematic representation of the system is provided in Figure 1. In brief, two translation stages were perpendicularly positioned on top of a worktop. A rectangular aluminum plate (45 × 25 mm) attached to the vertical stage has the role of the hard palate and was coupled with a three-axis force sensor (K3D60a, ME Systeme, Hennigsdorf, Germany) with a measurement range of ±50 N and an accuracy of 1%. The manufacturer indicates a sensitivity to transverse forces (cross-talk) of 1% of the measuring range at full load. Fillets were made on the edges of the palate (radius 2 mm) so as to limit the risk of damaging the TMSs during friction phases. During the design of the system, the distance between the sensor and the surface of the palate on which friction operates was reduced as much as possible (approximately 3 cm), in order to limit undesired bending effects, induced by the moment arm which applies to the force sensor. Indeed, it is important to note that the technology of strain gauge sensors is based on the principle of deflecting under load. Specifications from the manufacturer indicate that this model has a deflection of 100 µm under full load (50 N) and here, the sensor was not used for more than 20% of its measurement range. Moreover, the level of normal load imposed in the present experiments leads to a deformation of the TMSs by several millimeters. Under these conditions, the inclination of the palate caused by the twisting of the sensor must have a limited impact on the contact, which remains distributed over the entire lower face of the palate plate. A tongue holder part (with a parallelepipedic cavity adjusted to the dimensions of the TMSs) was attached to the horizontal stage. Both translation stages are displacement-controlled. LabVIEW® software (N.I., Austin, Texas, USA) was used to (i) control and acquire the position of the translation stages undergoing imposed sequences of motions and (ii) acquire in real-time the data from the force sensors using a bridge module with a 25 kHz sampling rate (NI-9237, N.I., Texas, USA).

2.4. Friction test protocol

The full experimental protocol of a single tribological test is described hereafter. Before the start of a test, the TMS was removed from the water container in which it is kept for storage, and the excess water with which it is covered was removed with absorbent paper (KIMTECH Science, Kimberly-Clark Europe Limited, Surrey, UK). Then, after visually checking that there is no excess water left on the upper surface of the TMS nor on the paper, the TMS was positioned in the tongue holder of the tribological setup.

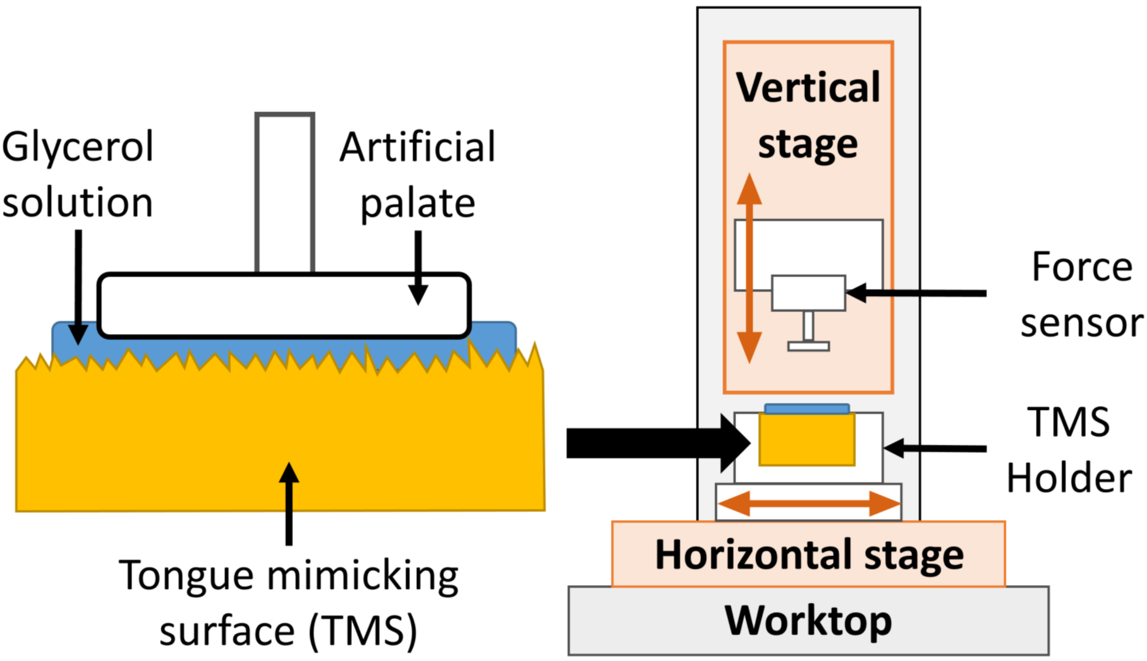

Figure 1. *Schematic representation of the custom-built tribometer. The lower part includes a TMS positioned on a horizontal translation stage (used to impose shearing movements). The upper part includes the rigid artificial palate and a force sensor, both mounted on a vertical translation stage (used to apply the normal force).*

A volume of 0.25 mL of a given glycerol solution was deposited on top of the TMS, in such a way that the solution would cover the whole surface area between the TMS and the aluminum plate playing the role of the palate, following previously established protocols [14]. Then, the aluminum plate was lowered until flush with the surface of the TMS, allowing to ensure the regular distribution and the spreading of glycerol solutions, with some excess expelled all around the aluminum plate's sides. Finally, the artificial palate was again lowered, until reaching a target value of normal force equal to 10 N (~9 kPa stress, based on the aluminum plate geometry). As the maximum compressive force between the tongue and the palate has been estimated at between 30 and 70 kPa [39,40], the value of normal load retained here seems relevant, especially for a product that does not need to be crushed. Once this starting position was reached, the testing sequence protocol was triggered without delay. The test protocol consisted of repeating a cycle five times during which shearing motions alternated with rest steps, in the absence of vertical motions. Figure 2 (a) represents the measurements of the variations of the position of the horizontal translation stage as a function of time during a cycle. The absence of curvature during the transient phases of acceleration and deceleration of the stage reveals that these phases are very short, both with respect to the scale of the duration of a cycle of movements and with respect to the kinetics of evolution of the measured forces. The four steps of a cycle are labeled in different colors and consist in what follows:

- Step #1: the horizontal translation stage moves forward in a total of 10 mm distance with a constant shearing velocity of 10 $mm.s^{-1}$;

- Step #2: a first holding step is observed for 1.5 s, with both stages held stationary;

- Step #3: the horizontal translation stage moves back to its initial position with the same constant shearing velocity of 10 $mm.s^{-1}$;

- Step #4: a second holding step is observed for 1.5 s.

While tongue velocity can be up to 200 $mm.s^{-1}$ [11], the velocity usually associated with liquid food consumption was for its part shown to be less than 30 $mm.s^{-1}$ [41]. The operational parameter of shearing velocity chosen for the experiments on the tribometer is thus relevant to conditions during normal eating.

For each TMS and each solution investigated, six replications were done on the tribological setup. All tribological measurements were done at room temperature (20 °C). The current version of the custom-built tribometer does not yet allow measurements under physiologically relevant temperatures (around 35°C in the oral cavity), therefore imposing to work at ambient laboratory temperature (20°C). This difference has consequences on the viscosity of the solutions, and therefore potentially on the characteristics of the contact. However, the diversity of glycerol solutions considered here makes it possible to cover a large part of the broad spectrum of viscosities encountered in oral conditions.

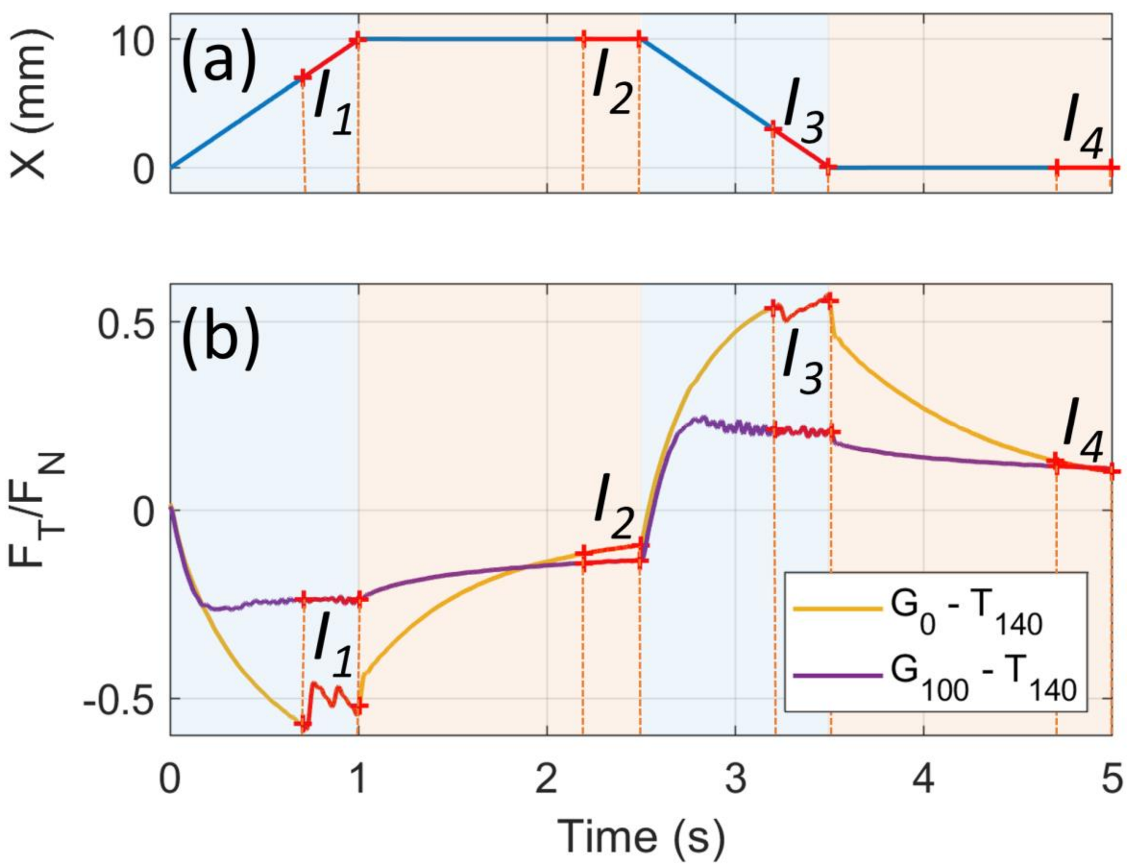

Figure 2. *(a) Displacement of the horizontal translation stage during one out of the five cycles composing a tribological test. (b) Corresponding curves of the ratio between tangential and normal forces provided in the case of TMS T_{140} (molded on P_{36} sandpaper) for two conditions of lubrication: G_0 in yellow and G_{100} in purple. Motion steps (rest steps, respectively) are represented on a blue (orange, respectively) background. The solid red lines delimited by red dotted vertical lines at the end of each step mark the intervals on which the analysis of the force ratio signal was focused in the paper: I_1 and I_3 at the end of motion steps, I_2 and I_4 at the end of rest steps.*

2.5. Processing and analysis of tangential to normal force ratio

The analysis of the signals recorded from the force sensor was performed using MATLAB (The MathWorks, Natick, Massachusetts, USA). The analysis was focused on the channels corresponding to normal and tangential loads. The signal processing is described schematically in Figure 3. It compiles the exhaustive description of the different processing steps allowing to obtain several quantitative indicators of interest from the raw signals. The following text takes them up step by step.

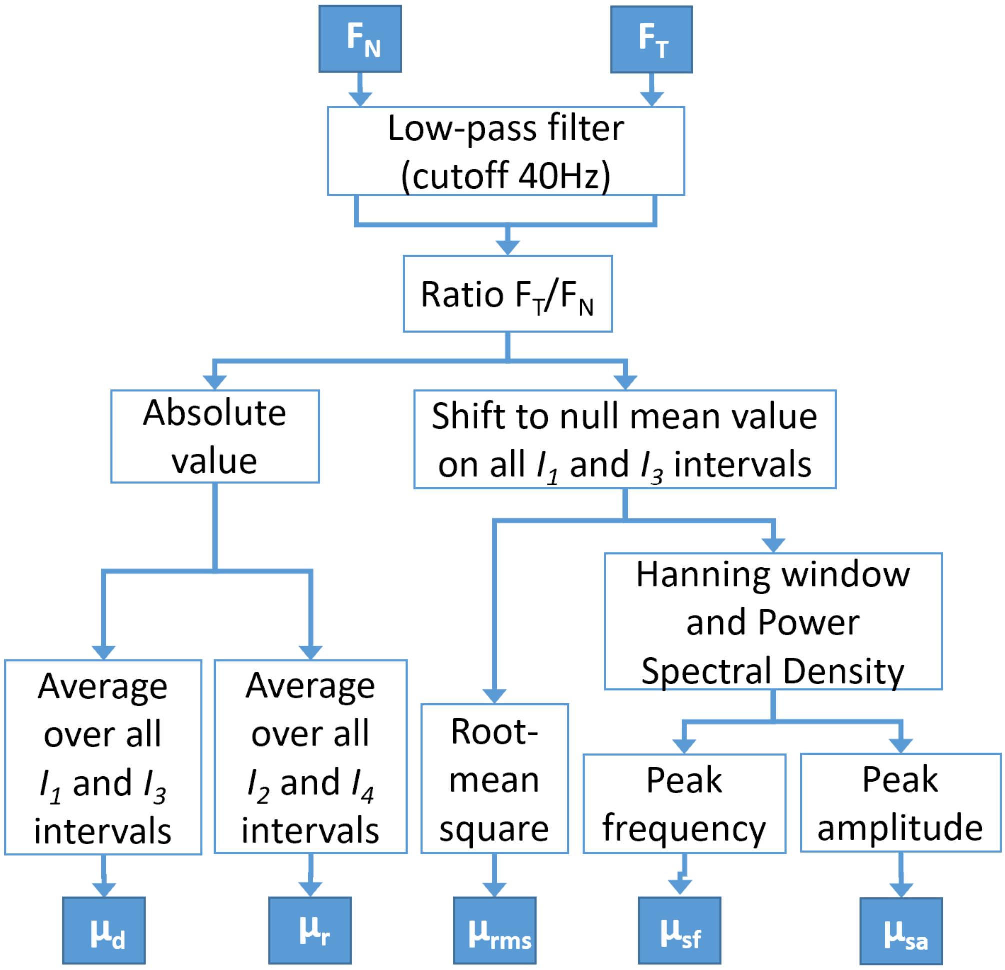

Figure 3. *Block diagram of the different signal processing steps followed to derive the five quantitative friction parameters discussed in the present study from the raw signals of force measured during the experiments.*

At first, to improve the signal-to-noise ratio and to eliminate undesirable components such as oscillations corresponding to 50 Hz power supply, a low pass filter (infinite impulse response filter, 6^{th} order, cut-off 40 Hz) was applied to all normal (F_N) and tangential (F_T) force signals. The cut-off frequency was determined based on the Fourier spectrum of raw force signals acquired in the absence of mechanical stresses. The recorded bandwidth (0-40 Hz) thus makes it possible to keep the dynamic information consistent with the technology of the strain gauge sensors used. However, it is important to note that applying a filter at such a low frequency loses a lot of information that would be relevant to the range of sensitivity of the mechanoreceptors of the tongue. Exploring frequency bands that are more representative of the sensitivity range of mechanoreceptors will thus require the use of other methodologies in the future.

Then, a particular effort was devoted to the analysis of the ratio between tangential and normal forces (directly related to friction). Figure 2 (b) shows examples of the evolution of the ratio between tangential and normal forces (F_T/F_N) during the first cycle of a test sequence (TMS molded with P_{36} sandpaper) for two conditions of lubrication: G_0 in (b) and G_{100} in (c). These examples are representative of the diversity of the trends observed throughout the different tested conditions (which are all provided separately in Figure 4). Quantitative information was extracted from the amplitude of this ratio, focusing on time windows defined at the end of each of the four steps composing a cycle. They are represented in red color in Figure 2. A compromise had to be found between time windows as large as possible to contain a maximum of information on the fluctuations of F_T/F_N, but also sufficiently narrow to ensure encompassing a period of time during which the average level of F_T/F_N tends to reach a plateau and therefore varies moderately. The duration of these intervals (0.3 s) was set based on the overall observation of the trends of all the tests, and after a series of attempts of calculation with different duration values. For each step of each cycle, the average values of $|F_T/F_N|$ (absolute value of F_T/F_N) over the corresponding time windows were determined (time windows I_1, I_2, I_3, and I_4 for steps #1, #2, #3, and #4, respectively). A preliminary analysis of these average values showed that there was no benefit in studying separately the information related to the forward and backward motions (either the motion steps #1 and #3 or the consecutive rest steps #2 and #4), nor to study a possible evolution of these mean values cycle after cycle during a test. In all cases, the differences or variations were not significant with respect to the intervals formed by the standard deviations. Consequently, it was decided to calculate, for each test, the average of the absolute value of the F_T/F_N ratio of (i) all the forward and backward motion step intervals (I_1 and I_3) and (ii) all the rest step intervals (I_2 and I_4). In what follows, the obtained average ratios during motion steps are referred to as μ_d (“d” for dynamic), while the average ratios during rest steps are referred to as μ_r (“r” for residual).

The fluctuations over time in F_T/F_N ratio were studied on the time intervals I_1 and I_3 (0.3 s at the end of motion steps #1 and #3). For each time interval, a shift to a null mean value was first applied. As an example, Figure 5 displays all the shifted signals for the first interval I_1. A first indicator was then built based on the root-mean-square (RMS) of the obtained signals. This indicator describes in a global way the amplitude of the fluctuations of F_T/F_N. In addition, a frequency spectrum calculation was performed by computing the power spectral density of all the time windows I_1 and I_3, applied after windowing by a Hanning window. The amplitude and the frequency of the peak of the spectrum between 0 and 40 Hz were extracted (bandwidth of the noise reduction low pass filter described above). In a very similar way to what was done for the calculations of μ_d, for each test, mean values of the parameters of RMS, frequency, and amplitude of the spectrum peak were calculated over all the time intervals I_1 and I_3 composing a test (see Figure 3). The resulting indicators are referred hereafter to as μ_{rms}, μ_{sf}, and μ_{sa} (for root mean square, spectrum frequency, and spectrum amplitude, respectively).

The mean values and standard deviations of each of the parameters studied (μ_d, μ_r, μ_{rms}, μ_{sf}, and μ_{sa}) were calculated over the six repetitions performed for any given set of conditions. Results were represented in the form of histograms or plots of the mean values of these repetitions, for which the error bars correspond to the standard deviations. Data analysis and graphical visualizations were done with MATLAB (The MathWorks, Natick, Massachusetts, USA).

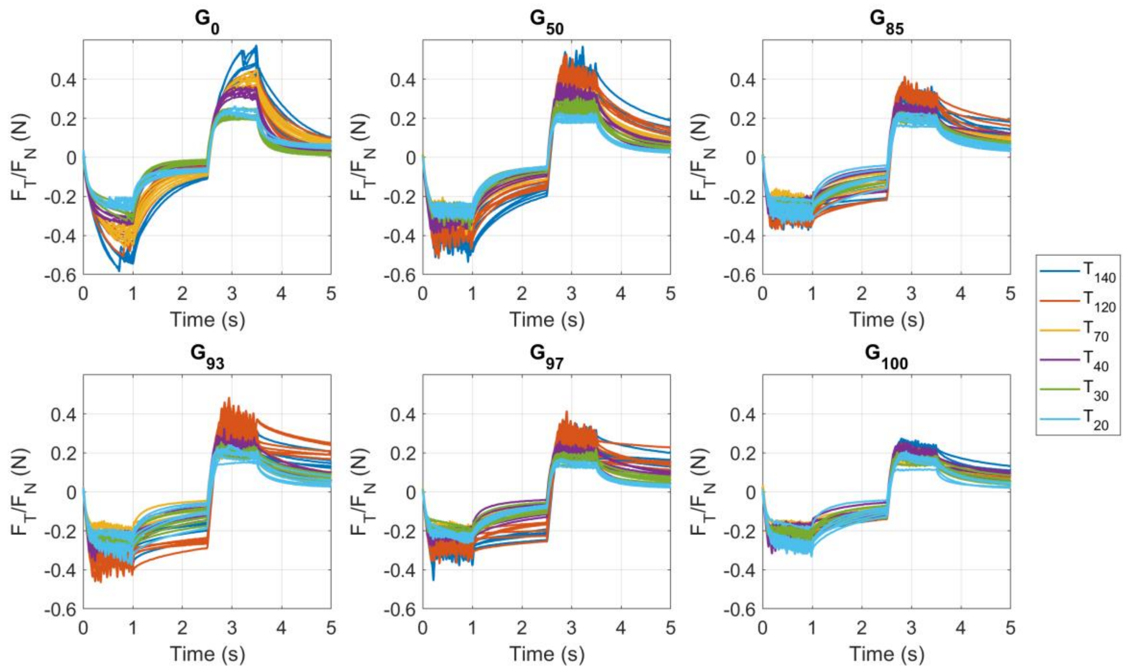

Figure 4. *Evolution of F_T/F_N as a function of time during the first cycle of the different tribological tests conducted with different lubrication conditions (one plot for each of the six solutions) and different TMSs (one color per type of TMS).*

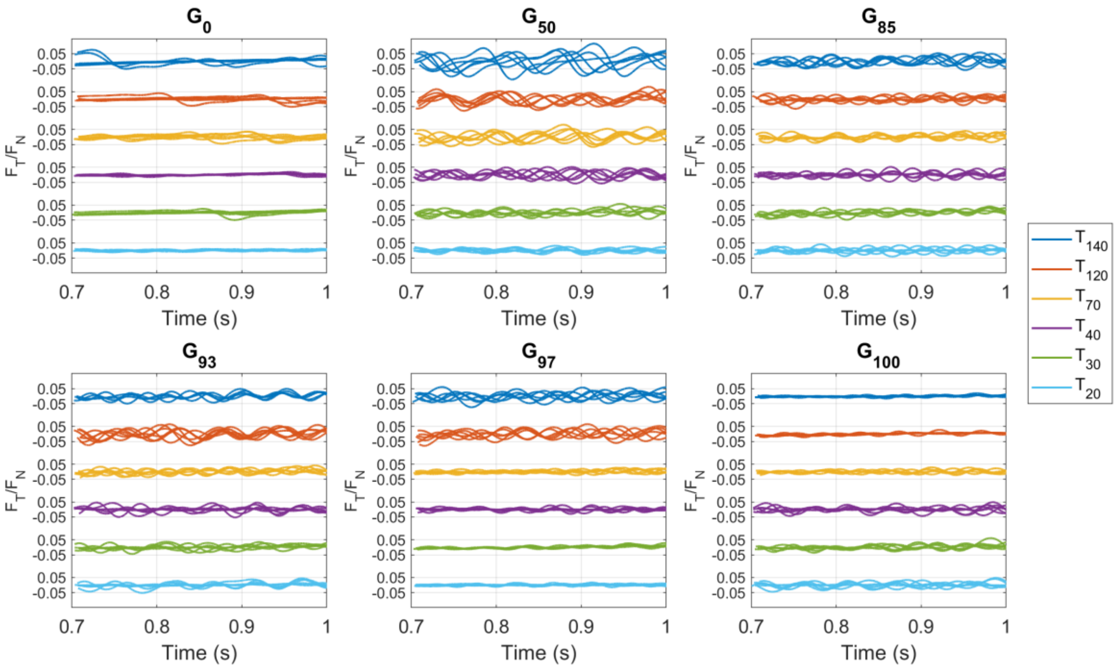

Figure 5. *F_T/F_N ratio as a function of time during the interval I_1 (0.3 s before the end of the first shearing motion) of the first cycle of a tribological test. Each box corresponds to a specific glycerol solution, while the colors detailed in the legend correspond to the different TMSs. The signals were shifted to have a null mean value and then to facilitate the comparison of the levels of fluctuations of F_T/F_N across the different conditions.*

3. Results and discussion

This results and discussion section first focuses on the characterization of the roughness of the TMSs, which is the factor having received the most extensive attention for the objectives of this study. The discussion then revolves around the results of the tribology measurements carried out by implementing the different roughness properties under variable lubrication conditions. These tribological results are discussed in two separate sub-sections. The first sub-section is dedicated to the analysis of the average level of amplitude of the ratio F_T/F_N during the motion and the rest steps (related to μ_d and μ_r, respectively). The second focuses on the fluctuations of the ratio F_T/F_N during the motion steps (with the analysis of μ_{rms}, μ_{sf}, and μ_{sa}), and their complementarity with the amplitude measurements discussed in the previous section.

3.1. Roughness properties of the TMSs

The topography of the TMSs was characterized in order to analyze (i) the impact of the imprint material used in the molding process (sandpapers or silicone sheet) on the height and width of TMSs asperities, and (ii) the physiological relevance of obtained roughness properties. The average and standard deviation values of Ra and RSm parameters, obtained on the six types of TMSs, are represented in the form of histograms in Figure 6. The legends in the abscissa axis correspond to the materials used to imprint the roughness to the TMSs: five abrasive paper references (P_{24}, P_{36}, P_{40}, $P_{80,}$ and P_{100}) and a silicone sheet (Sil). Quite expectantly, the general trend was that the higher the SEPA class of sandpaper roughness (from rough P_{24} to smooth P_{100} sandpaper), the lower the obtained values of Ra and RSm. If RSm values seem to correspond well to the grit size of the sandpapers, the Ra values are for their part an order of magnitude lower. Shrinking phenomena previously evidenced for PVA artificial tongues [14] may explain the discrepancy between sandpaper grit size and Ra values. When looking closer, the TMS prepared with P_{36} sandpaper class had a higher asperity height Ra than the TMS prepared with the roughest sandpaper (P_{24}). Differences in the wetting abilities of the abrasive surfaces by the PVA solution might be expected according to the roughness characteristics of the sandpaper. For rough surfaces, air might be entrapped at the bottom of the valleys of the asperities, affecting the resulting roughness of the print. These observations show the importance of characterizing the TMSs after their manufacturing, as the reliable reproduction of the roughness of the molds is a very complex task.

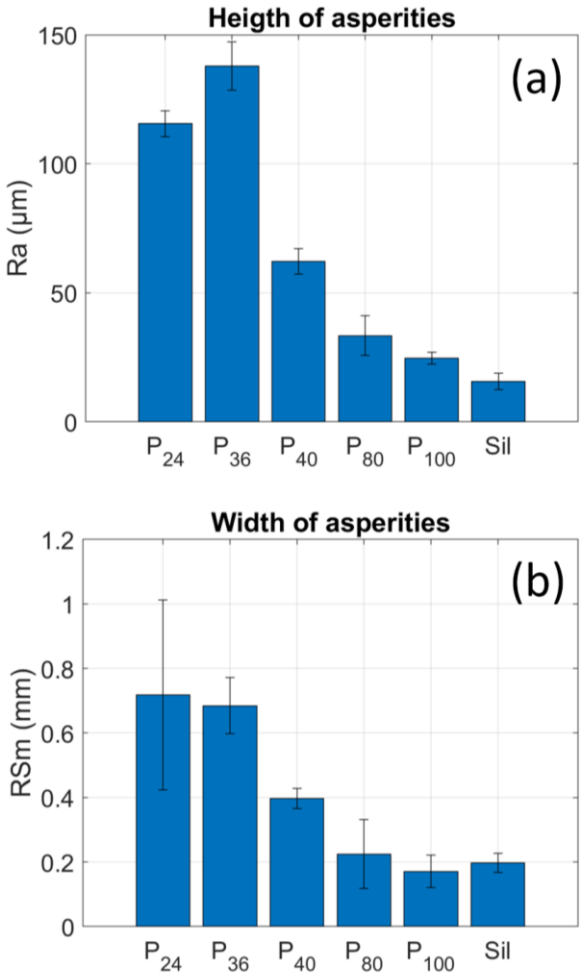

Figure 6. *Mean and standard deviation values of Ra and RSm roughness parameters, measured for six types of TMSs: five were molded on sandpaper sheets (from P_{24} to P_{100}) while the last one was molded on a silicone sheet (Sil).*

The two parameters Ra and RSm were shown to follow similar trends across the different TMSs. As Ra is generally considered as the reference roughness property in the literature, in the rest of the manuscript, the six types of TMSs have been labeled according to their average Ra value (rounded up to the next ten microns): T_{20}, T_{30}, T_{40}, T_{70}, T_{120}, and T_{140}. Table 2 provides the correspondence between the name given to each TMS, the material on which they were molded (silicone or sandpaper), the grit size in the case of sandpaper (according to the SEPA classification), and the mean and standard deviation values of Ra and RSm actually measured. Hereafter, the results will be systematically presented by classifying the TMSs in increasing order of the mean Ra value.

Table 2. *Table of the different TMSs, indicating their names, the material on which they were molded (silicone or sandpaper), the grit size in the case of sandpaper (according to the SEPA classification), and the average and standard deviation values of Ra and RSm actually measured.*

TMS label	T_{20}	T_{30}	T_{40}	T_{70}	T_{120}	T_{140}
Imprint material	Silicone	P_{100}	P_{80}	P_{40}	P_{24}	P_{36}
Grit size (µm)	-	160	200	400	750	550
Ra (µm)	16 ± 3	25 ± 2	33 ± 8	67 ± 5	116 ± 5	138 ± 9
RSm (µm)	198 ± 3	171 ± 5	225 ± 1	397 ± 3	718 ± 2	685 ± 8

Figure 7 shows the 2-D images of profilometry obtained on the six types of TMSs. They make it possible to qualitatively confirm, from T_{20} to T_{140}, the increase in the height and width of the asperities, consistently with the measured values of Ra and RSm. Nevertheless, it is noticeable that the qualitative differences in visual appearance between the TMSs T_{20} and T_{30} are more pronounced than what the gap of measured values of Ra and RSm would suggest. One hypothesis that could explain this is that for low roughness levels, the cut-off length λ_c of the applied pre-processing filters is less suitable for separating the roughness and waviness components of the profiles. The reliability of the values of the resulting roughness parameters can thus be affected. Subsequently, in the following, we will therefore keep in mind that the TMS T_{20} (made from a silicone sheet) is smoother than the TMS T_{30} (obtained from P_{100}, the smoothest of the five types of sandpapers).

The average values of Ra ranged from 15.6 to 137.9 µm, and were thus shown to be physiologically relevant after comparison with *in vivo* measurements from the literature. Such measurements are particularly complex *in situ* because the surfaces to characterize are difficult to access and pose great technical problems because of their irregularity and their high deformability. Most studies rely on the *ex situ* analysis of casts, which raises the question of potential loss of information between the roughness properties of the reference surface (that one wishes to characterize) and those from the molds on which the measurements are actually carried out. This challenge has been tackled by several teams who have conducted essential work to characterize the orders of magnitude of the height of human tongue asperities in recent publications. The distribution of the height of tongue asperities could thus be estimated to range from 20.9 to 121.9 µm in a first study including 58 participants [42], and from 40.0 to 160.0

µm in a more recent one with 71 volunteers [36]. Differences could also be noticed between fungiform (390.0 ±72.0 µm) and filiform (195.0 ±30.0 µm) papillae [37]. Although presenting slight differences attributable to the technical difficulties mentioned above and to inter-individual variability, these precious orders of magnitude turn out to be in good agreement with the measurements carried out on the TMSs of the study, thus validating their physiological relevance. The analysis of the tribology results below is thus based on experiments carried out under topographical conditions consistent with the physiological environment.

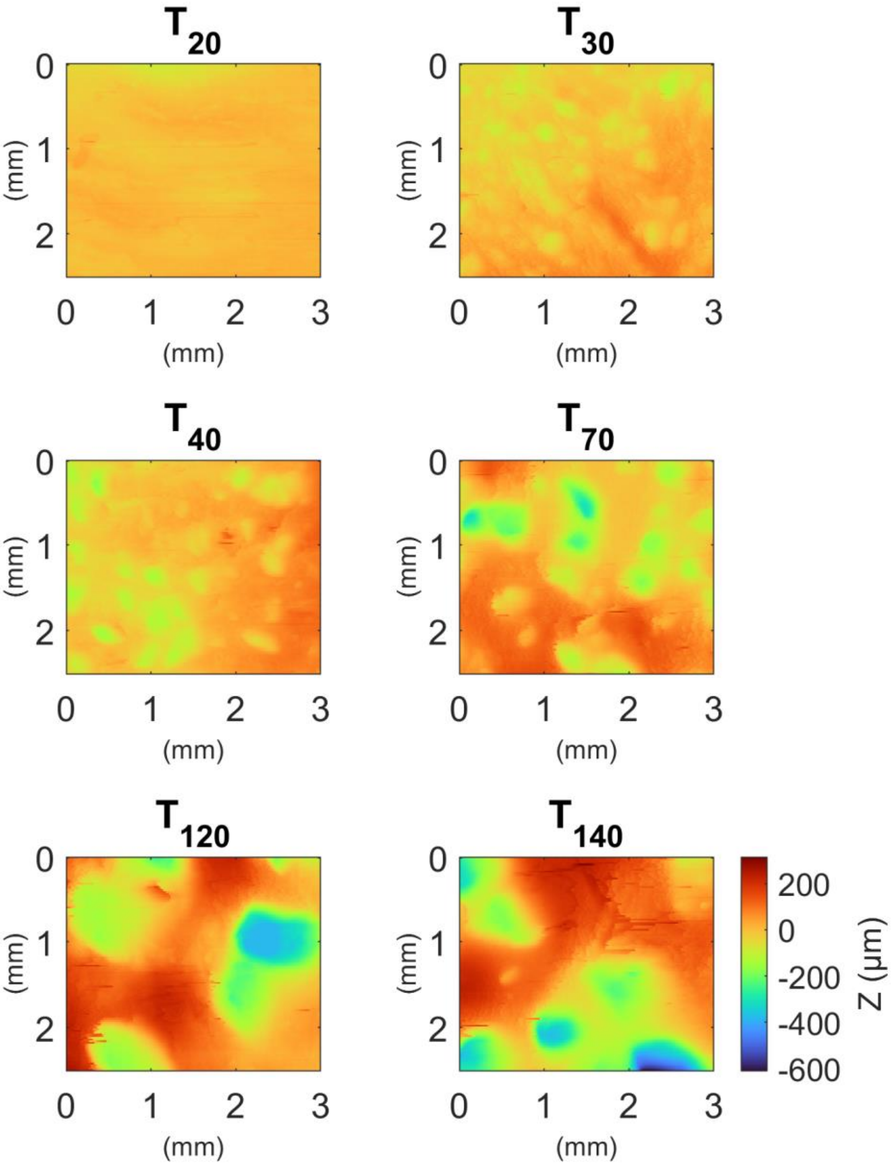

Figure 7. *2-D images of profilometry obtained on the six types of TMSs, where the height of the profile is coded in color.*

3.2. Impact of TMS roughness on friction amplitude levels

Figure 2 (b) represents the evolution of F_T/F_N as a function of time during the first cycle for two tests conducted on the roughest TMS, but with different lubrication conditions: pure water (G_0) in yellow, and pure glycerol (G_{100}) in purple. These examples illustrate the diversity of the trends observed throughout the different tested conditions, which are all available in Figure 4. During the motion steps (between 0 and 1 s and between 2.5 and 3.5 s), two well-known phases of evolution of the ratio between tangential and normal forces may be distinguished. During the first phase (which can be referred to as static phase), a progressive increase in $|F_T/F_N|$ may reflect the elastic deformations undergone in the bulk of TMSs when the slip threshold has not been crossed. This phase may therefore depend on the rigidity of the TMS and on the level of adhesion between the surfaces of the TMS and of the palate. The second phase (referred to as dynamic phase) may correspond to crossing of the friction cone. The sliding between the palate and the TMS then occurs (stick-slip), while the ratio F_T/F_N fluctuates around a plateau value (which corresponds to what is called friction coefficient). The duration of these two phases varies greatly across the different experimental conditions. Figure 2 (b) shows two of the most distinct scenarios that can be observed on the entire dataset, both obtained with the roughest TMS (T_{140}). On these examples, lubrication with thin G_0 led to a high level of friction reached at the end of a long static phase. Contrarily, lubrication with thick G_{100} displayed a low level of friction after a short static phase. Hereafter, friction analysis was focused on the plateau values of $|F_T/F_N|$ reached at the end of the motion and rest steps of the tests (μ_d and μ_r).

3.2.1. Friction levels in two extreme cases of lubrication

The behavior of coefficients μ_d (magnitude of $|F_T/F_N|$ at the end of motion steps) and μ_r (at the end of the rest steps) will first be discussed in the two extreme cases of lubrication by pure water and pure glycerol (G_0 and G_{100}). In Figure 8, the average values of μ_d and μ_r have been plotted as a function of the mean Ra roughness values measured on the different TMSs.

Lubrication with the most viscous solution (G_{100}) led to the lowest values of μ_d, with, if any, a moderate roughness dependence observed across the six TMSs. Combined with the short durations of static friction phases observed during the motion steps and already reported in the raw curves provided in Figure 4, these observations suggest that the hydrodynamic lift exerted by G_{100} may be high enough to avoid any direct contact between the asperities of the TMSs and the palate plate (for these conditions of shearing velocity and normal force). The most probable hypothesis is thus that under these conditions, the system gets close to the hydrodynamic regime. Contrastingly, lubrication with the thinnest solution (G_0) led to an increase of μ_d with roughness, starting from a low level close to that of G_{100} for the smoothest TMS and moving away from it as the TMSs become rougher. This increase of μ_d with roughness may be associated with an increase of the effective area of contact between the asperities of the TMS and the palate. Such trends are thus consistent with the mixed regime of lubrication.

If μ_d coefficient can be directly compared to the friction coefficient commonly assessed with commercial tribometers, the residual friction level μ_r characterized during rest steps is less classic. Food oral processing being composed of alternating phases of motion and rest, following the evolution of the friction ratio F_T/F_N during motionless steps may also provide relevant information about tongue-food-palate mechanical interactions (with consequences on texture perception). The originality of this custom-built tribometer is that it offers complete freedom in the sequences of movements to impose, with the access to full raw data for analyzing force signals at any time during a test. For each individual condition of lubrication and roughness, μ_r was found to be lower than μ_d, reflecting the tendency of the system to adapt itself to the mechanical stresses applied during the motion steps. These particular plots do not make it possible to identify a clear trend of dependence of μ_r on the roughness of the TMSs or on the type of lubricant. Indeed, independently from the level of friction reached at the end of a shear motion, rest periods generally enabled the recovery of similar residual levels of $|F_T/F_N|$ before moving to the next motion step. The amplitude of the decrease of $|F_T/F_N|$ observed both for G_0 and G_{100} during rest steps could thus be directly linked to the magnitude reached at the end of motion steps. When shear motions are stopped, the hydrodynamic pressure exerted by the fluid at the interface suddenly drops. The fluid in question then flows out of the space under the palate plate and at least part of the asperities of the TMS comes into direct contact with the plate. Resulting adhesion between the TMS and the palate may lead to residual stresses within the TMS, which can give rise to mechanical relaxation phenomena.

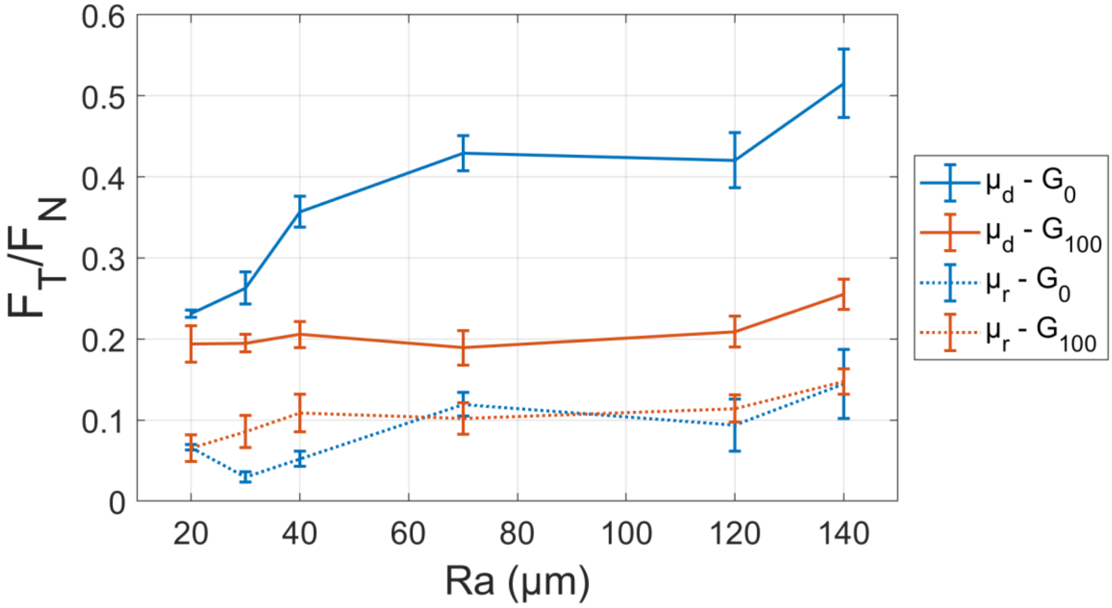

Figure 8. *Average and standard deviation values of friction parameters μ_d (during motion steps) and μ_r (during rest steps) as a function of TMS roughness, for the two extreme cases of lubrication considered: G_0 and G_{100}.*

Based on the trends of μ_d and μ_r observed in the cases of lubrication with the thinnest and the thickest solutions, the following part of the discussion suggests taking a closer look at what happens when the viscosity is gradually varied. Indeed, fixing normal stress and shearing velocity and varying the viscosity as it has been done here is one of the possible strategies to progressively investigate transitions through lubrication regimes [43]. Mixtures of glycerol and water were considered here as they are commonly used in classical tribological investigations for the construction of Stribeck curves [44], and they make it possible to cover much of the spectrum of viscosity properties of the liquid foods we consume. It is also interesting to note that the literature reports that from 80 to 100% glycerol concentration, reorganizations take place in the solutions, resulting in a sharp increase in compressibility [45].

3.2.2. Friction levels in intermediate cases of lubrication

Figures 9 (a) and (b) represent the variations of μ_d and μ_r as a function of lubricant viscosity for the six TMSs. From the smoothest to the roughest TMS, an increased dependence of μ_d on viscosity is observed, with a decreasing trend which may be characteristic of the mixed regime of lubrication. As the TMSs become smoother, an attenuation of the decay of μ_d is observed, with μ_d levels becoming lower. Such trend may suggest that for smoother TMSs, the system reaches the transition phase between mixed and hydrodynamic regimes.

Concerning the residual friction level μ_r, no clear trends of viscosity-dependence could be identified. As already observed in Figure 8, each condition plotted in Figures 9 (a) and (b) shows a value of μ_r lower than its corresponding one of μ_d. Interestingly, it can be noted that the curves of the six TMSs are ranked in the same order in Figures 9 (a) and (b): the smoother the TMS, the lower the levels of μ_d and μ_r. Figure 9 (c) illustrates the possible relations between μ_d and μ_r by plotting them against each other for each test performed. The points of the same color correspond to all the tests carried out with the same TMS (all lubrication conditions combined). The general scatter plot obtained does not seem to reveal a simple relationship between the two parameters. As the values of μ_d increase, the range of observed values for μ_r also increases. The residual level of friction at the end of the rest steps cannot therefore be explained solely by the amplitude of the level reached at the end of the motion steps. Looking color by color (meaning roughness by roughness), we see that the measurement points corresponding to the two smoothest TMSs (T_{20} and T_{30}) group together in a limited space corresponding to the lowest values of μ_r and μ_d observed in the entire dataset. Conversely, for rougher TMSs (from T_{40} to T_{140}, which cover more closely the topographic characteristics of the human tongue), much wider ranges of μ_d and μ_r values could be observed. As a consequence, for this range of roughness properties, the information provided by the two friction parameters μ_d and μ_r is not redundant, but complementary.

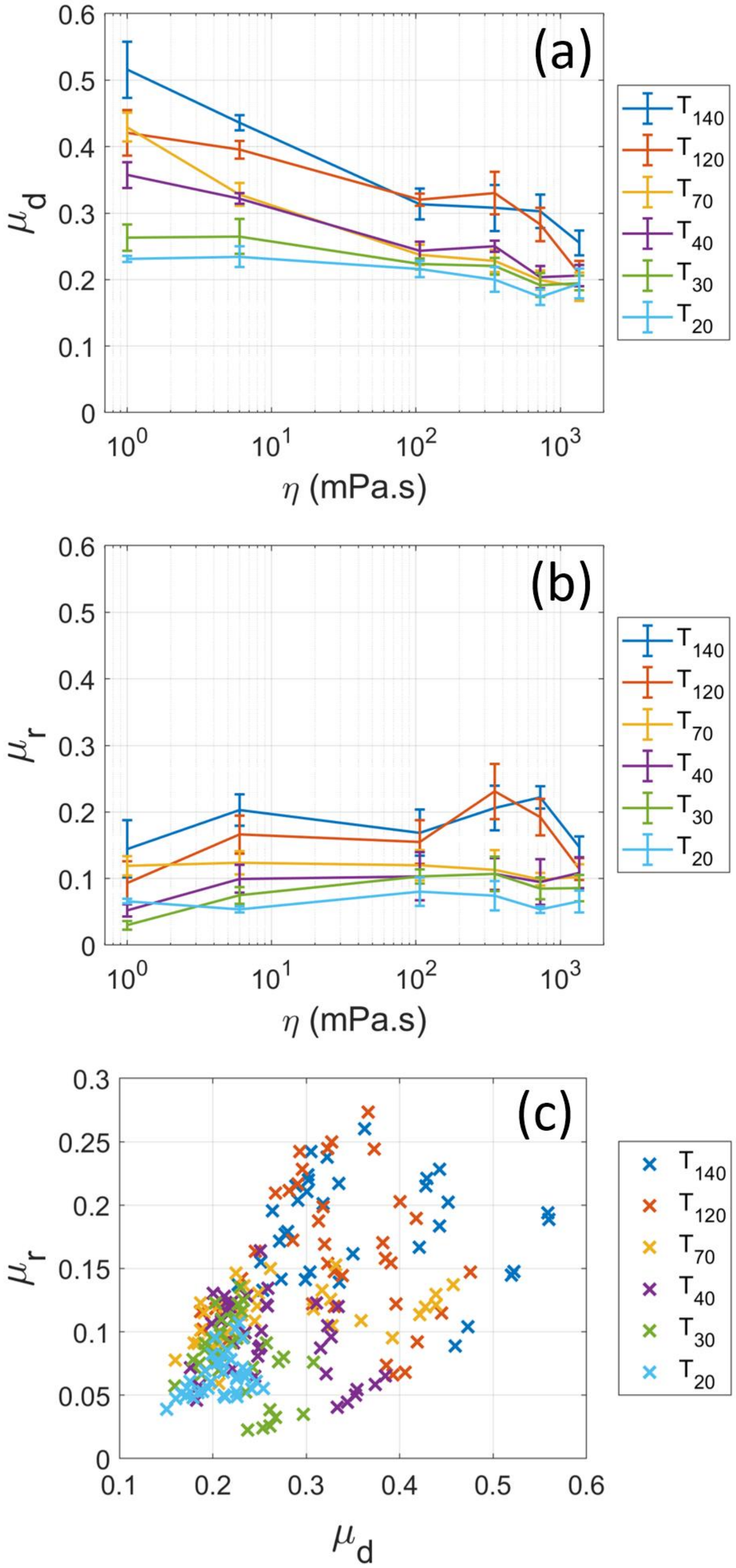

Figure 9. *Average and standard deviation values of μ_d (a) and μ_r (b) as a function of lubricant visocity for the six TMSs. In (c), μ_d and μ_r values plotted against each other for each test performed, with points of the same color corresponding to tests carried out with the same TMS (all lubrication conditions combined).*

3.3. Fluctuations of friction levels during motion steps

Most conventional tribology tools limit the analysis of force signals to the calculation of the friction coefficient, which is calculated over time intervals during which shears forces are high enough to induce sliding between the tribopairs, as done in the present study with parameter μ_d. However, the ratio F_T/F_N evolves all along the time windows on which μ_d is calculated, and such dynamic behavior also deserves attention. Sanahuja et al. [32] have highlighted with originality the importance of produced stick-slip effects resulting from intermittent sliding motions during dynamic friction. These phenomena result in fluctuations in the signal of the ratio between tangential and normal forces, the analysis of which unfortunately remains too rare in the literature. Figure 5 gathers all the signals of F_T/F_N acquired at the end the first shearing movement applied (shifted to a null mean value). This time window is the first out of the ten time windows used for the calculation of μ_d. Varied behaviors of fluctuations in F_T/F_N could be reported across the different lubrication and roughness conditions. Such fluctuations may carry information about the influence of tongue roughness and lubrication on intermittent adhesion and sliding events at tongue-palate interface. Quantitative parameters were thus built to analyze both the amplitude and the frequency of these fluctuations.

Figure 10 (a) describes the mean and standard deviation values of μ_{rms}, corresponding to the root-mean-square of F_T/F_N calculated on time windows I_1 and I_3 (at the end of the motion steps). For most of the lubrication conditions considered, the general trend observed was that the rougher the TMS, the higher the reported levels of μ_{rms}. This tendency of the dependence of μ_{rms} on the roughness of the TMSs supports the hypothesis that the level of normal force applied in the present experiments is not sufficient to completely deform and flatten the asperities of the TMSs. The importance of the intermittence of contact and slip events at the interface between the TMS and the palate testified by the high levels of μ_{rms} is characteristic of the mixed lubrication regime. However, when considering each TMS individually, the impact of the viscosity of glycerol is more complex to conclude on. The smoother the TMS, the higher the reproducibility of the measurements (shorter error bars), the lower the amplitude of μ_{rms}, and the lower the differences reported across the six solutions. Conversely, the rougher the TMS, the lower the reproducibility but the higher the diversity of amplitude levels of μ_{rms} observed across the lubrication conditions. Interestingly, although G_0 and G_{100} have been shown to display the most contrasting levels of μ_d, they behaved similarly with respect to μ_{rms}. Indeed, both conditions led to the lowest levels of μ_{rms}, with low variations across the different TMSs. Oppositely, G_{50} led to the highest levels of μ_{rms} reported on each of the TMSs, even though it has a viscosity close to that of G_0 and it gave values of μ_d also close to those of G_0. These discrepancies between the trends observed for the parameters μ_d and μ_{rms} are therefore interesting to highlight through the comparison figure of μ_{rms} versus μ_d proposed in Figures 10 (b). The measurement points of the two smoothest TMSs (T_{20} and T_{30}) are gathered in a restricted space combining low values of magnitude of friction level (μ_d) and low amplitudes of friction fluctuations (μ_{rms}). For rougher TMSs, higher levels were generally observed for these two parameters, without being able to identify a clear trend of proportionality. This plot highlights the complementarity of the friction parameters μ_d and μ_{rms}, and thus shows the interest in extending the tribological characterizations beyond the friction coefficient alone.

It is interesting to relate these observations to the mechanisms of tactile perceptions. Mechanoreceptors are specialized receptors connected with neural endings and are found in human tissues such as skin and also in oral mucosa tissues among which, of course, the tongue. They can detect mechanical stimuli that cause deformations or some sort of distortions on the tissue surface and translate them into electrical signals to the brain. One report described three types of receptors in the tongue: SA1 is responsible for the form and texture of food, FA1 detects low-frequency vibrations, and SA2 detects tongue position and shape [46]. It is then very interesting to underline that each piece of information brought by μ_d, μ_r, and μ_{rms} can be associated with different types of sensory stimuli for different mechanoreceptors: slowly adapting mechanoreceptors produce sustained responses to static stimulation (proportional to the applied level of stress), while rapidly adapting mechanoreceptors produce transient responses to the sudden changes in stress levels. Fluctuations characterized by μ_{rms} could therefore be particularly relevant for understanding the impacts of rapidly adapting receptors. To determine the major frequencies encountered across these fluctuations, and their impact on the global signal, the frequency response of the signals has been investigated.

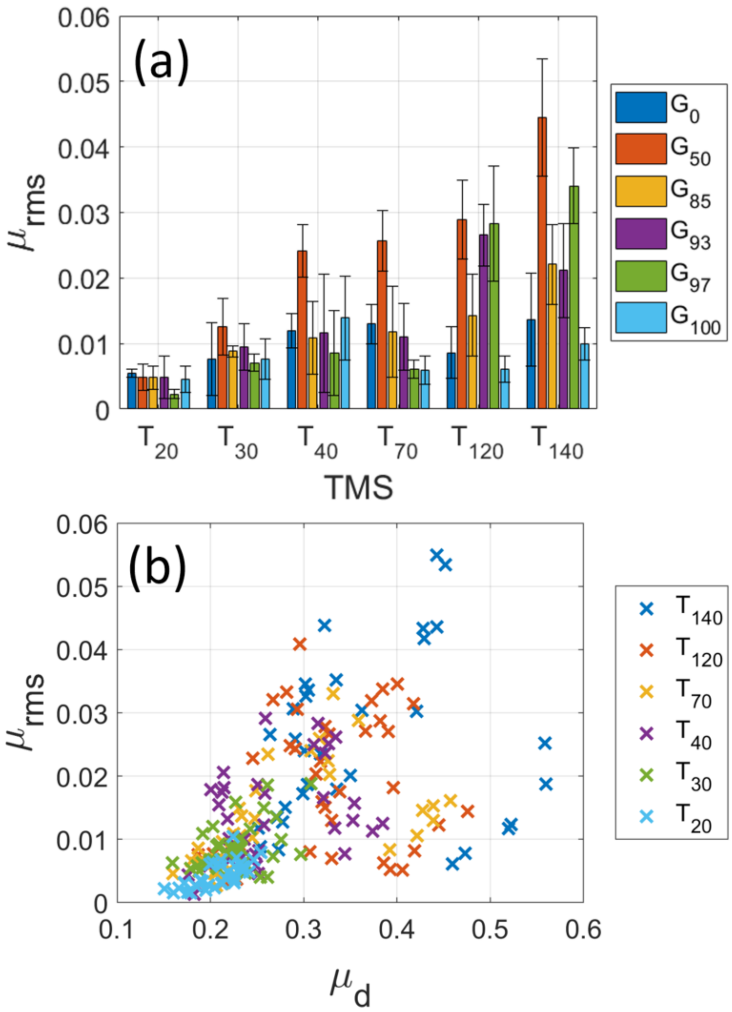

Figure 10. *(a) Average and standard deviation values of the root mean square* μ_{rms} *of* F_T/F_N *during the 0.3 s before shear motions end. (b)* μ_{rms} *and* μ_d *values plotted against each other for each test performed, with points of the same color corresponding to tests carried out with the same TMS (all lubrication conditions combined).*

Figures 11 (a) and (b) describe the mean and standard deviation values of the frequency (μ_{sf}) and the amplitude (μ_{sa}) associated with the peak of the frequency spectrum of F_T/F_N signals (taken from the 0.3 s before shear motions end) on all I_1 and I_3 intervals. The results show that μ_{sf} (frequency at which the spectrum peak amplitude occurs) does not vary significantly between the different roughness conditions. Except for the results obtained on G_0 (lowest viscosity) which show lower frequencies, the average frequencies ranged between 10 and 20 Hz, without clear trends or statistical differences between the different roughness and lubrication conditions. A relationship between this frequency μ_{sf} and the characteristic width of the asperities of the TMSs (RSm) could have been expected, but this is not the case. This absence of relationship could be due to the random nature of the spatial distribution of the asperities. Indeed, as the asperities do not have a periodic arrangement with respect to the direction in which the shearing movement is operated, the alternations of the sliding and sticking phases might not take place in phase with the width of the asperities. Furthermore, the low pass filter at 40 Hz that had to be applied to the signals significantly reduces the frequency content that can be analyzed. The range of sensitivity attributed to the mechanoreceptors present in the tissues of oral mucosa is much broader (0.3 to 400 Hz) [32,47–50]. Although already providing interesting information with sensors that are not entirely suitable, the study shows the interest in using sensor methods dedicated to vibration analysis.

The general shape of the plot related to the peaks of spectrum amplitude μ_{sa} (Figure 11 (b)) is for its part very similar to that obtained for the average level μ_{rms} (Figure 10 (a)), with a general tendency for μ_{sa} to increase as the roughness of the TMSs increases. These results show that the amplitude of the fluctuations of F_T/F_N is essentially carried by the frequency component associated with the peak amplitude of the spectrum. Under these conditions, the relationship established in Figure 11 (c), where μ_{rms} and μ_{sa} are plotted against each other, only reflects the mathematical relationship between the amplitudes in the time and frequency domains.

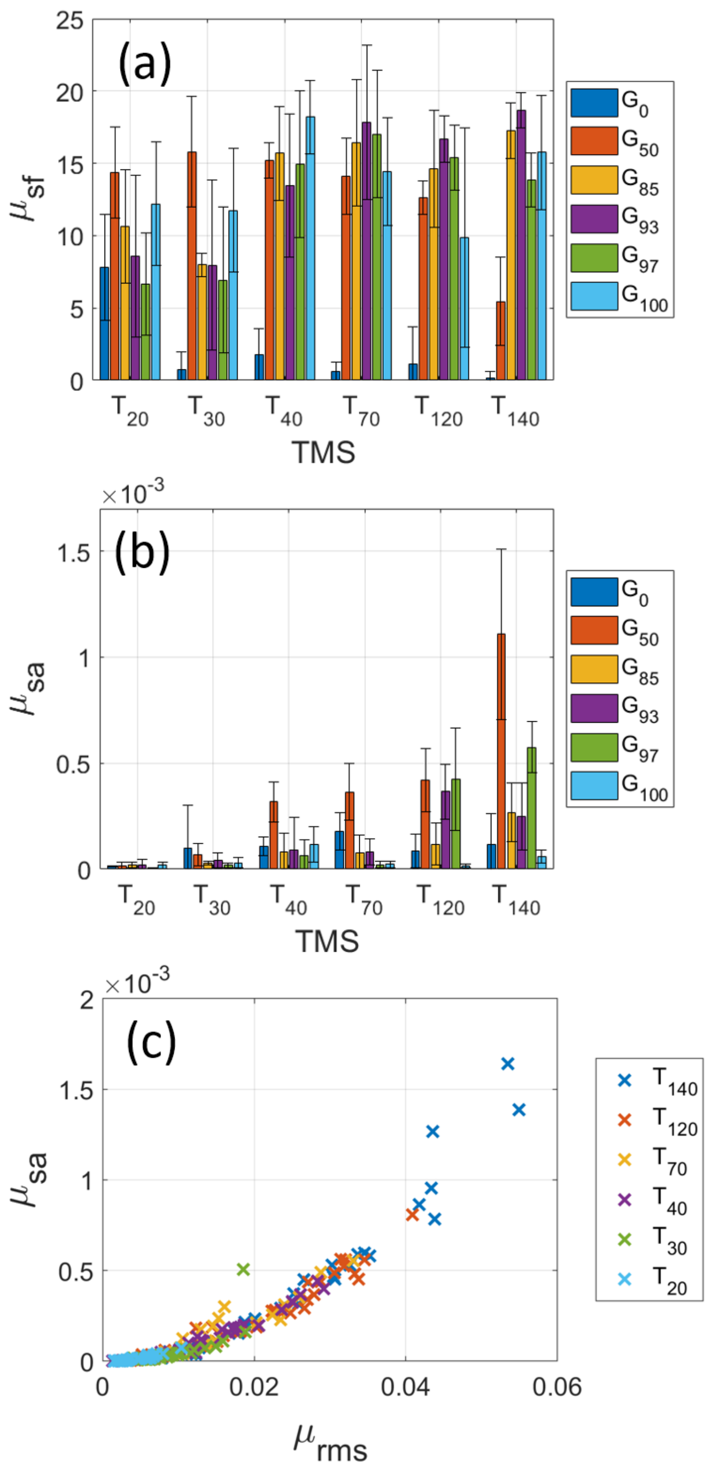

Figure 11. *Average and standard deviation values of the spectrum frequency μ_{sf} (in a), and of the spectrum amplitude μ_{sa} (in b) of F_T/F_N during the 0.3 s before shear motions end. (c) μ_{sa} and μ_{rms} values plotted against each other for each test performed, with points of the same color corresponding to tests carried out with the same TMS (all lubrication conditions combined).*

4. Conclusion

The artificial tongues made from PVA implemented on this custom-built tribometer confer the originality of being able to study the role of the roughness of the tongue by considering a tribopair with a physiologically relevant contact surface. Furthermore, the conduct of non-classical tribology test protocols (combining motion and rest steps) and the analysis of the raw data of the ratio between tangential and normal forces constitute another point of originality. Here, the average values of friction level observed at the end of motion steps were found to increase when (i) the roughness of the TMSs increased and when (ii) the viscosity of glycerol solutions decreased. These trends could be consistent with mixed lubrication. The decrease of friction level during rest steps showed a potential to monitor mechanical relaxation in the bulk of the TMSs. Finally, the fluctuations of friction level during motion steps were for their part generally of higher amplitude as the roughness of the surface increased. In the future, alternative methodologies may help to study these phenomena of fluctuations in wider frequency bands (more representative of mechanoreceptor sensitivity). By going further than the analysis of the friction coefficient to which tribology studies are often restricted, the study shows that deeper analyses of the signal of the friction level may therefore provide additional knowledge, that could contribute to a better understanding of the mechanisms of texture perception.

In future works, the development of theoretical models could be considered, in order to attempt to predict the evolutions of the thickness of the lubricating film and of the morphology of the asperities of the TMSs as a function of time during the experiments. The identification of the lubrication regimes at which the system operates could thus be confirmed with more certainty.

As food oral processing cannot be represented just by pure shear back-and-forth motions as considered here for validation purposes, future work will require the usage of the full capacity of the custom-built tribometer. Complex sequences of motions combining compression and shear can indeed be imposed, and the behavior of normal and tangential forces will be investigated under these conditions (both in terms of amplitude and of fluctuations). Future experiments will also consist of accounting for the tongue lubrication with human or artificial saliva, and investigating the behavior of more complex model foods, ranging from semi-liquid to semi-solid products, with various degrees of heterogeneity. The validation of this newly designed system may thus open up many opportunities for aiding in the development of novel food products adapted to the physiology of specific populations.

5. Credit author statement

Miodrag Glumac: Conceptualization, Methodology, Validation, Formal analysis, Investigation, Resources, Data curation, Writing – original draft, Writing – review & editing, Visualization

Véronique Bosc: Conceptualization, Writing – Review & Editing

Paul Menut: Conceptualization, Writing – Review & Editing

Marco Ramaioli: Conceptualization, Writing – Review & Editing

Frédéric Restagno: Conceptualization, Ressources, Writing – Review & Editing

Sandrine Mariot: Investigation, Ressources, Writing – Review & Editing

Vincent Mathieu: Conceptualization, Methodology, Software, Validation, Formal analysis, Investigation, Resources, Data curation, Writing – original draft, Writing – review & editing, Visualization, Supervision, Project administration, Funding acquisition

6. Funding

This work was financially supported by the QUSToFood project funded by the French National Research Agency (ANR-17-CE21-004).

7. Declaration of interest

The authors have no conflicting financial or any other interests to declare.

8. Acknowledgements

The authors wish to acknowledge the crucial technical support provided by David Forest.

9. References

[1] A.S. Szczesniak, Texture is a sensory property, Food Quality and Preference. 13 (2002) 215–225. https://doi.org/10.1016/S0950-3293(01)00039-8.

[2] Chen, Food oral processing-A review, Food Hydrocolloids. 23 (2009) 1–25. https://doi.org/10.1016/j.foodhyd.2007.11.013.

[3] J.R. Stokes, M.W. Boehm, S.K. Baier, Oral processing, texture and mouthfeel: From rheology to tribology and beyond, Current Opinion in Colloid and Interface Science. 18 (2013) 349–359. https://doi.org/10.1016/j.cocis.2013.04.010.

[4] E.C. Ketel, R.A. de Wijk, C. de Graaf, M. Stieger, Relating oral physiology and anatomy of consumers varying in age, gender and ethnicity to food oral processing behavior, Physiology and Behavior. 215 (2020) 112766. https://doi.org/10.1016/j.physbeh.2019.112766.

[5] S. Panda, J. Chen, O. Benjamin, Development of model mouth for food oral processing studies: Present challenges and scopes, Innovative Food Science and Emerging Technologies. 66 (2020) 102524. https://doi.org/10.1016/j.ifset.2020.102524.

[6] S. Ishihara, S. Nakao, M. Nakauma, T. Funami, K. Hori, T. Ono, K. Kohyama, K. Nishinari, Compression Test of Food Gels on Artificial Tongue and Its Comparison with Human Test, Journal of Texture Studies. 44 (2013) 104–114. https://doi.org/10.1111/jtxs.12002.

[7] W. Xu, S. Yu, M. Zhong, A review on food oral tribology, Friction. 10 (2022) 1927–1966. https://doi.org/10.1007/s40544-022-0594-9.

[8] Q. Wang, Y. Zhu, J. Chen, Development of a simulated tongue substrate for in vitro soft “oral” tribology study, Food Hydrocolloids. 120 (2021) 106991. https://doi.org/10.1016/j.foodhyd.2021.106991.

[9] A. Sarkar, E.M. Krop, Marrying oral tribology to sensory perception: a systematic review, Current Opinion in Food Science. 27 (2019) 64–73. https://doi.org/10.1016/j.cofs.2019.05.007.

[10] C. Pradal, J.R. Stokes, Oral tribology: Bridging the gap between physical measurements and sensory experience, Current Opinion in Food Science. 9 (2016) 34–41. https://doi.org/10.1016/j.cofs.2016.04.008.

[11] A. Sarkar, E. Andablo-Reyes, M. Bryant, D. Dowson, A. Neville, Lubrication of soft oral surfaces, Current Opinion in Colloid and Interface Science. 39 (2019) 61–75. https://doi.org/10.1016/j.cocis.2019.01.008.

[12] H.M. Shewan, C. Pradal, J.R. Stokes, Tribology and its growing use toward the study of food oral processing and sensory perception, Journal of Texture Studies. 51 (2020) 7–22. https://doi.org/10.1111/jtxs.12452.

[13] R.E. Rudge, E. Scholten, J.A. Dijksman, Advances and challenges in soft tribology with applications to foods, Current Opinion in Food Science. 27 (2019) 90–97. https://doi.org/10.1016/j.cofs.2019.06.011.

[14] R. Srivastava, V. Bosc, F. Restagno, C. Tournier, P. Menut, I. Souchon, V. Mathieu, A new biomimetic set-up to understand the role of the kinematic, mechanical, and surface characteristics of the tongue in food oral tribological studies, Food Hydrocolloids. 115 (2021). https://doi.org/10.1016/j.foodhyd.2021.106602.

[15] P. Kuchaiyaphum, G. Rifai, W. Yuuki, T. Yamauchi, Hyaluronic acid-poly(vinyl alcohol) composite cryo-gel for biofunctional material application, Polymers for Advanced Technologies. 30 (2019) 94–100. https://doi.org/10.1002/pat.4447.

[16] S. Tsui, J. Tandy, C. Myant, M. Masen, P.M. Cann, Friction measurements with yoghurt in a simulated tongue-palate contact, Biotribology. 8 (2016) 1–11. https://doi.org/10.1016/j.biotri.2016.02.001.

[17] M.A. van Stee, E. de Hoog, F. van de Velde, Oral Parameters Affecting Ex-vivo Tribology, Biotribology. 11 (2017) 84–91. https://doi.org/10.1016/j.biotri.2017.05.001.

[18] O. Torres, A. Yamada, N.M. Rigby, T. Hanawa, Y. Kawano, A. Sarkar, Gellan gum: A new member in the dysphagia thickener family, Biotribology. 17 (2019) 8–18. https://doi.org/10.1016/j.biotri.2019.02.002.

[19] H. Cai, Y. Li, J. Chen, Rheology and Tribology Study of the Sensory Perception of Oral Care Products, Biotribology. 10 (2017) 17–25. https://doi.org/10.1016/j.biotri.2017.03.001.

[20] A. Araiza-Calahorra, A.R. Mackie, G. Feron, A. Sarkar, Can tribology be a tool to help tailor food for elderly population?, Current Opinion in Food Science. 49 (2023) 100968. https://doi.org/10.1016/j.cofs.2022.100968.

[21] B.L. Miles, Z. Wu, K.S. Kennedy, K. Zhao, C.T. Simons, Elucidation of a lingual detection mechanism for high-viscosity solutions in humans, Food and Function. 13 (2022) 64–75. https://doi.org/10.1039/d1fo02460d.

[22] X.X. Wang, J. Chen, X.X. Wang, In situ oral lubrication and smoothness sensory perception influenced by tongue surface roughness, Journal of the Science of Food and Agriculture. 102 (2022) 132–138. https://doi.org/10.1002/jsfa.11339.

[23] M. Mantelet, R. Srivastava, F. Restagno, I. Souchon, V. Mathieu, Real time ultrasound assessment of contact progress between food gels and tongue mimicking surfaces during a compression, Food Hydrocolloids. 109 (2020). https://doi.org/10.1016/j.foodhyd.2020.106099.

[24] M. Mantelet, F. Restagno, I. Souchon, V. Mathieu, Using ultrasound to characterize the tongue-food interface: An in vitro study examining the impact of surface roughness and lubrication, Ultrasonics. 103 (2020) 106095. https://doi.org/10.1016/j.ultras.2020.106095.

[25] A. Araiza-Calahorra, A.R. Mackie, G. Feron, A. Sarkar, Can tribology be a tool to help tailor food for elderly population?, Current Opinion in Food Science. 49 (2023) 100968. https://doi.org/10.1016/j.cofs.2022.100968.

[26] T. Tominaga, T. Kurokawa, H. Furukawa, Y. Osada, J.P. Gong, Friction of a soft hydrogel on rough solid substrates, Soft Matter. 4 (2008) 1645–1652. https://doi.org/10.1039/b802568a.

[27] S. Yashima, N. Takase, T. Kurokawa, J.P. Gong, Friction of hydrogels with controlled surface roughness on solid flat substrates, Soft Matter. 10 (2014) 3192–3199. https://doi.org/10.1039/c3sm52883a.

[28] R.E.D. Rudge, E. Scholten, J.A. Dijksman, Natural and induced surface roughness determine frictional regimes in hydrogel pairs, Tribology International. 141 (2020) 105903. https://doi.org/10.1016/j.triboint.2019.105903.

[29] R. Rudge, E. Scholten, J.A. Dijksman, A matter of morphology: The role of asperity characteristics in hydrogel friction, Tribology International. 174 (2022) 107694. https://doi.org/10.1016/j.triboint.2022.107694.

[30] B.L. Taylor, T.B. Mills, Surface texture modifications for oral processing applications, Biotribology. 23 (2020) 100132. https://doi.org/10.1016/j.biotri.2020.100132.

[31] L.M.C. Collins, C. Dawes, The Surface Area of the Adult Human Mouth and Thickness of the Salivary Film Covering the Teeth and Oral Mucosa, Journal of Dental Research. 66 (1987) 1300–1302. https://doi.org/10.1177/00220345870660080201.

[32] S. Sanahuja, R. Upadhyay, H. Briesen, J. Chen, Spectral analysis of the stick-slip phenomenon in “oral” tribological texture evaluation, Journal of Texture Studies. 48 (2017) 318–334. https://doi.org/10.1111/jtxs.12266.

[33] M.L. Sheely, Glycerol Viscosity Tables, Industrial and Engineering Chemistry. 24 (1932) 1060–1064. https://doi.org/10.1021/ie50273a022.

[34] Jason R. Stokes, Principles and Practices of Instrumental Characterisation for Eating and Sensory Perception Studies, in: Jianshe Chen, L. Engelen (Eds.), Food Oral Processing: Fundamentals of Eating and Sensory Perception, 1st ed., Blackwell Publishing Ltd, John Wiley & Sons, Ltd, The Atrium, Southern Gate, Chichester, West Sussex, PO19 8SQ, UK, 2012: pp. 227–263.

[35] A.A. Aleksandrov, M.S. Trakhtengerts, Viscosity of water at temperatures of -20 to 150°C, Journal of Engineering Physics. 27 (1974) 1235–1239. https://doi.org/10.1007/BF00864022.

[36] X. Wang, X. Wang, R. Upadhyay, J. Chen, Topographic study of human tongue in relation to oral tribology, Food Hydrocolloids. 95 (2019) 116–121. https://doi.org/10.1016/j.foodhyd.2019.04.022.

[37] E. Andablo-Reyes, M. Bryant, A. Neville, P. Hyde, R. Sarkar, M. Francis, A. Sarkar, 3D Biomimetic Tongue-Emulating Surfaces for Tribological Applications, ACS Applied Materials and Interfaces. 12 (2020) 49371–49385. https://doi.org/10.1021/acsami.0c12925.

[38] P. Giusti, L. Lazzeri, N. Barbani, P. Narducci, A. Bonaretti, M. Palla, L. Lelli, Hydrogels of poly(vinyl alcohol) and collagen as new bioartificial materials - Part I Physical and morphological characterization, Journal of Materials Science: Materials in Medicine. 4 (1993) 538–542. https://doi.org/10.1007/BF00125590.

[39] W.A. Alsanei, J. Chen, Studies of the Oral Capabilities in Relation to Bolus Manipulations and the Ease of Initiating Bolus Flow, Journal of Texture Studies. 45 (2014) 1–12. https://doi.org/10.1111/jtxs.12041.

[40] L. Laguna, R.A. Barrowclough, J. Chen, A. Sarkar, New Approach to Food Difficulty Perception: Food Structure, Food Oral Processing and Individual's Physical Strength, Journal of Texture Studies. 47 (2016) 413–422. https://doi.org/10.1111/jtxs.12190.

[41] C. Peng, P.-G. Jost-Brinkmann, R.-R. Miethke, C.-T. Lin, Ultrasonographic Measurement of Tongue Movement During Swallowing, Journal of Ultrasound in Medicine. (2000) 15–20. https://doi.org/10.7863/jum.2000.19.1.15.

[42] N. Uemori, Y. Kakinoki, J. Karaki, H. Kakigawa, New method for determining surface roughness of tongue, Gerodontology. 29 (2012) 90–95. https://doi.org/10.1111/j.1741-2358.2011.00509.x.

[43] Y. Xu, B. Cartwright, L. Advincula, C. Myant, J.R. Stokes, Generalised scaling law for soft contact tribology: Influence of load and asymmetric surface deformation, Tribology International. 163 (2021) 107192. https://doi.org/10.1016/j.triboint.2021.107192.

[44] J.M. Kim, F. Wolf, S.K. Baier, Effect of varying mixing ratio of PDMS on the consistency of the soft-contact Stribeck curve for glycerol solutions, Tribology International. 89 (2015) 46–53. https://doi.org/10.1016/j.triboint.2014.12.010.

[45] L. Negadi, B. Feddal-Benabed, I. Bahadur, J. Saab, M. Zaoui-Djelloul-Daouadji, D. Ramjugernath, A. Negadi, Effect of temperature on density, sound velocity, and their derived properties for the binary systems glycerol with water or alcohols, Journal of Chemical Thermodynamics. 109 (2017) 124–136. https://doi.org/10.1016/j.jct.2017.01.011.

[46] L. Engelen, Oral Receptors, in: J. Chen, L. Engelen (Eds.), Food Oral Processing: Fundamentals of Eating and Sensory Perception, 1 st ed., Blackwell Publishing Ltd, 2012: pp. 15–43. https://doi.org/10.1002/9781444360943.

[47] N. Asamura, N. Yokoyama, H. Shinoda, Selectively stimulating skin receptors for tactile display, IEEE Computer Graphics and Applications. 18 (1998) 32–37. https://doi.org/10.1109/38.734977.

[48] F. Shao, X.J. Chen, C.J. Barnes, B. Henson, A novel tactile sensation measurement system for qualifying touch perception, Proceedings of the Institution of Mechanical

Engineers, Part H: Journal of Engineering in Medicine. 224 (2010) 97–105. https://doi.org/10.1243/09544119JEIM658.

[49] G.A. Van Aken, Modelling texture perception by soft epithelial surfaces, Soft Matter. 6 (2010) 826–834. https://doi.org/10.1039/b916708k.

[50] R. Upadhyay, N. Brossard, J. Chen, Mechanisms underlying astringency: Introduction to an oral tribology approach, Journal of Physics D: Applied Physics. 49 (2016) 104003. https://doi.org/10.1088/0022-3727/49/10/104003.